Superconducting three-dimensional networks in a magnetic field: Frustrated systems

Osamu Sato*
Department of Liberal Arts, Osaka Prefectural College of Technology, Neyagawa, Osaka 572-8572, Japan

Suminobu Takamori
Department of Mathematical Sciences, Osaka Prefecture University, 1-1, Gakuencho, Sakai, Osaka 599-8531, Japan

Masaru Kato†
Department of Mathematical Sciences, Osaka Prefecture University, 1-1, Gakuencho, Sakai, Osaka 599-8531, Japan
and CREST, JST, 4-1-8, Honcho, Kawaguchi, Saitama 332-0012, Japan
(Received 10 October 2003; published 16 March 2004)

Making use of the de Gennes–Alexander network equation, we have investigated the transition temperature of three-dimensional superconducting networks in a magnetic field. For the magnetic field $H(0.75<Ha^2/\Phi_0<2.25)$, a superconducting tetrahedron has a nonsuperconducting vertex because of the frustration. In contrast to this, the C60 fullerene network shows antifluxons when the magnetic field is normal to one of the pentagons and hexagons, because of the frustration that comes from the rotational symmetry around these polygons.

DOI: 10.1103/PhysRevB.69.092505 PACS number(s): 74.81.Fa, 74.20.De, 74.25.Qt

Multiply connected type-I superconductors shows a peculiar response to the external magnetic field. This is because magnetic flux can go through the holes of the superconductors in the unit of the flux quanta without much loss of energy and the magnetic flux through the hole causes the winding of the phase θ of the superconducting order parameter $\Delta=|\Delta|e^{i\theta}$. This is in contrast to the complete Meissner state of the simply connected type-I superconductors. A simple example is the Little-Parks experiment,[1,2] which shows periodic variation of transition temperature of the superconducting cylinder as a function of the magnetic field which is parallel to the cylinder.

Superconducting networks are extreme examples of them. They consist of connected superconducting wires. Theoretical studies of superconducting networks began with de Gennes' work[3] on the superconducting lasso under magnetic field. The subsequent work of Alexander[4] generalized de Gennes' method which is an application of the linearized Ginzburg-Landau (GL) equation, to the general superconducting networks. This is called the de Gennes–Alexander network equation.

The two-dimensional networks are studied theoretically[5–9] and experimentally[10–20] because they can be made from the superconducting films. From the viewpoint of the multiple connectivity, however, we can expect three-dimensional superconducting networks to show other peculiar behaviors. In the case of three-dimensional networks, because quantized flux must go inside through one of the faces and go out through another, if the areas of two faces are different, it causes a different frustration. Also there are several symmetry axes for different kinds of rotation around them. Symmetry of the superconductors causes frustration under a magnetic field and induces unusual magnetic flux structures. For example, an antivortex and giant vortex appear in mesoscopic superconducting plate for suitable external magnetic field.[21–23]

In this Brief Report we propose three-dimensional superconducting networks and study their transition temperature and structure of magnetic flux in a magnetic field. As a candidate of three-dimensional networks, we consider a tetrahedral network and a fullerene (C60) network. In these networks, only their edges are superconductors.

A tetrahedron is the simplest symmetrical polyhedron, which consists of three triangles. It has a threefold rotational symmetry around an axis that is normal to the one of the face and goes through the opposite vertex. C_{60} fullerene is a truncated icosahedron. This truncated icosahedron has 12 pentagons and 20 hexagons. Its geometry has many symmetrical axes. Around an axis that is normal to a pentagon and through the center of the fullerene, there is fivefold rotational symmetry. Also around the axis of a hexagon that is the same as the pentagon, there is threefold symmetry and around an axis that goes through the center of an edge that is shared by adjacent two hexagons, there is twofold symmetry. The symmetries of the two networks make the magnetic flux structure complex.

In the following we only consider the vicinity of the transition temperature of networks in a magnetic field, therefore the linearized Ginzburg-Landau equation is applicable. Also we assume that the diameter of the wires is small compared to the GL coherence length $\xi(T)$ and the penetration depth λ. Then the order parameter and the magnetic field are uniform across the cross section of the wires. We rotate the applied magnetic field from the normal direction of the basal plane. We define this applied field and its vector potential as

$$\boldsymbol{H}=(H\sin\theta\cos\phi, H\sin\theta\sin\phi, H\cos\theta), \tag{1}$$

$$\boldsymbol{A}=\frac{H}{2}(z\sin\theta\sin\phi-y\cos\theta, x\cos\theta - z\sin\theta\cos\phi, y\sin\theta\cos\phi-x\sin\theta\sin\phi). \tag{2}$$

First we consider a tetrahedral network, as shown in Fig. 1(a). We denote the order parameter at each vertex 1, 2, 3, and 4 as Δ_1, Δ_2, Δ_3, and Δ_4.

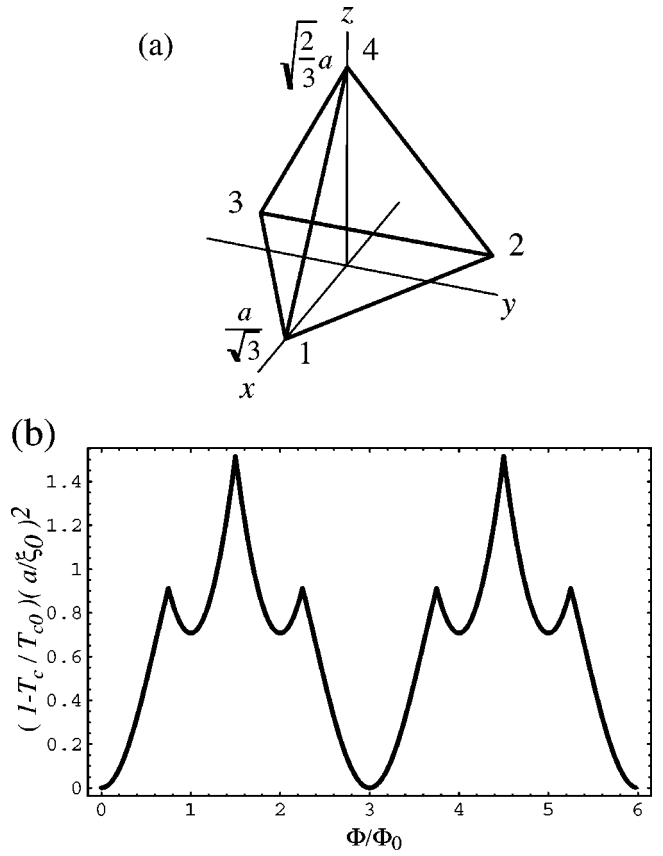

FIG. 1. (a) A tetrahedral network. 1–4 are indices of the vertex. a is the length of the bond. (b) Decrease of the transition temperature as a function of the magnitude of the external field when the field is parallel to z direction.

Then the de Gennes–Alexander equation is given as

$$3\cos\frac{a}{\xi(T)}\begin{pmatrix}\Delta_1\\ \Delta_2\\ \Delta_3\\ \Delta_4\end{pmatrix} = \begin{pmatrix} 0 & M_1 & M_1^* & M_2^* \\ M_1^* & 0 & M_1 & M_2M_3 \\ M_1 & M_1^* & 0 & M_2M_3^* \\ M_2 & M_2^*M_3^* & M_2^*M_3 & 0 \end{pmatrix}\begin{pmatrix}\Delta_1\\ \Delta_2\\ \Delta_3\\ \Delta_4\end{pmatrix}. \quad (3)$$

Here we define $M_1=e^{i\gamma\cos\theta}$, $M_2=e^{i\gamma 2\sqrt{2}\sin\theta\sin\phi/\sqrt{3}}$, and $M_3=e^{i\gamma\sqrt{2}\sin\theta\cos\theta}$, where $\gamma=2\pi\Phi/3\Phi_0$, $\Phi=H\sqrt{3}a^2/4$ is the flux through the basal triangle when the field is perpendicular to it, and $\Phi_0=hc/2e$ is a flux quantum.

Solving this equation as an eigenvalue problem, we get the eigenvalues $3\cos[a/\xi(T)]=3\cos(a\sqrt{1-T/T_{c0}}/\xi_0)$, where T_{c0} is the superconducting transition temperature of the bulk at zero field and ξ_0 is the coherence length at zero temperature. The largest eigenvalue is related to the transition temperature. We show the decrease of the transition temperature as a function of the magnitude of the external field in Fig. 1(b). The transition temperature is periodic with period $3\Phi_0$, because when $\Phi=3\Phi_0$, the magnetic flux through all of the triangle on the surface becomes a multiple of Φ_0. The fluxoid can be calculated from the order parameter.[9] The structure of the order parameter and the fluxoid vary with increasing applied field as shown in Fig. 2. When $\Phi/\Phi_0=1$, a quantum fluxoid goes through the basal triangle. But it cannot be divided to 1/3 quantum at upper three triangle surface, then the superconductivity is destroyed at the vertex 4. This state is stable until $\Phi/\Phi_0=1.5$. For $\Phi/\Phi_0>1.5$, the fluxoid that goes through the basal triangle becomes two flux quanta and the order parameter structure is similar to the previous state. These two states are not very stable at $\Phi/\Phi_0=1.5$, therefore the transition temperature becomes lowest at $\Phi/\Phi_0=1.5$.

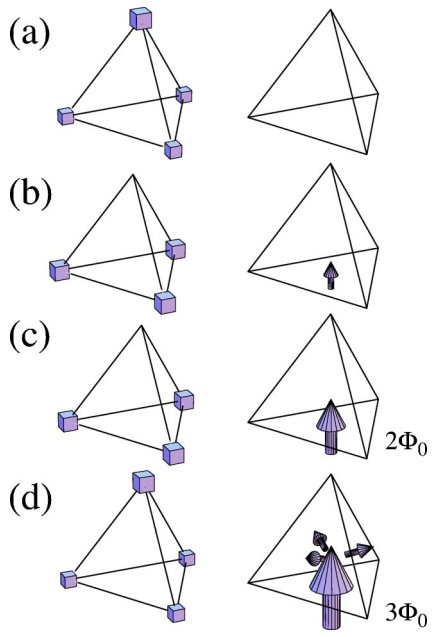

FIG. 2. Order parameter and fluxoid structure of the tetrahedral network for $\Phi/\Phi_0=0.5$ (a), $\Phi/\Phi_0=1.0$ (b), $\Phi/\Phi_0=2.0$ (c), and $\Phi/\Phi_0=2.5$ (d). In the left column, a cube shows the magnitude of the order parameter Δ_i at the vertex i. In the right column, an arrow shows the magnitude and direction of the fluxoid.

Dependence of the transition temperature on the direction of the applied field is shown in Fig. 3. The tetrahedron has threefold symmetry in the z direction, so the transition tem-

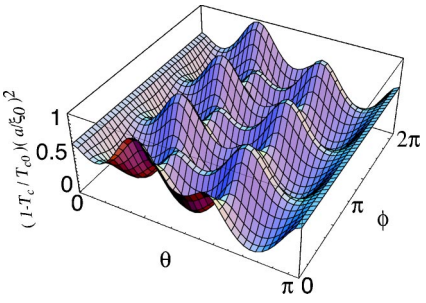

FIG. 3. The transition temperature as a function of the direction of the applied field. The magnitude of the applied field is set as $\Phi=\sqrt{3}Ha^2/4=\Phi_0$.

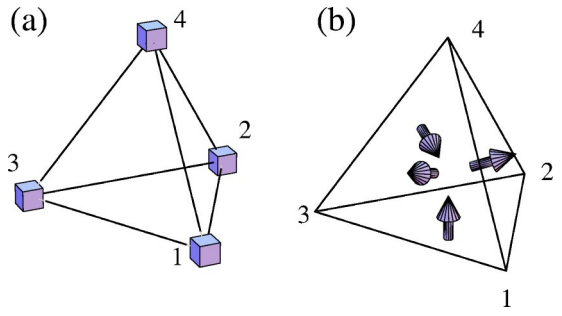

FIG. 4. The structure of the order parameter (a) and magnetic flux (b) for $\phi=0$, $\theta=\arccos(1/\sqrt{3})$ and $\Phi=\Phi_0$.

perature also shows threefold symmetry. Maximum destruction of the transition temperature occurs at $\phi=0$ and $\theta=\arccos(1/\sqrt{3})$, where the field is perpendicular to the edge 41. The structures of the order parameter and fluxoid for this case are shown in Fig. 4. In this state, the quantized fluxoid comes through each of two triangular faces 234 and 123 and goes out through each of other two faces 431 and 124.

Next we investigate a C60 fullerene superconducting network (C60SNW) in a magnetic field. Each of the vertices is connected to three vertices in the C60SNW as shown in Fig. 5. Therefore the de Gennes–Alexander equation for the C60SNW at a vertex i becomes as

$$\sum_{j=1}^{3} \Delta_j \exp(i\gamma_{i,j}) = 3\cos\frac{a}{\xi(T)}, \tag{4}$$

where

$$\gamma_{i,j} = \frac{2\pi}{\Phi_0}\int_{r_i}^{r_j} \boldsymbol{A}(\boldsymbol{r})\cdot d\boldsymbol{r}. \tag{5}$$

Here j denotes a vertex which is connected with the vertex i, $\boldsymbol{r}_i$ is the position of the vertex i, Δ_i is the order parameter of the vertex i, and a is the length of edges of C60SNW.

We now discuss the case where the direction of the external magnetic field is normal to a pentagon of C60SNW. By solving Eq. (4), we get the magnetic field dependence of the transition temperature and order parameters at 60 vertices. The transition temperature is shown in Fig. 6. Here we defined external magnetic flux per a pentagon, $\Phi=1.72a^2H$. The transition temperature curve is nonperiodic of Φ/Φ_0, because the ratio of projection areas of a pentagon to the normal plane of the external field and that of its neighboring

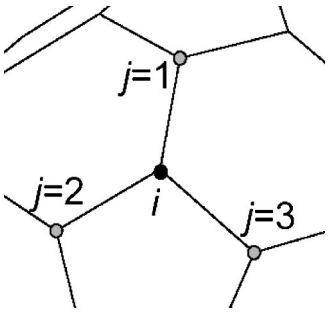

FIG. 5. A vertex point i and it's connected points j's.

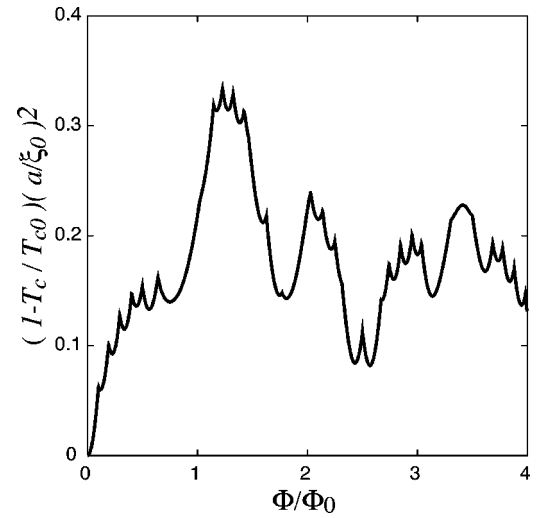

FIG. 6. The magnetic field dependence of decrease of the transition temperature when the field is perpendicular to a pentagon, where $\Phi=1.72a^2H$.

hexagons is irrational. Each of the dip structures in Fig. 6 corresponds to a different fluxon distribution structure where total magnetic flux through the networks increases monotonically and the cusps are the transition points between them.

Stable fluxon distributions of C60SNW for several external fields are shown in Fig. 7. Each distribution holds five-fold rotational symmetry around a pentagon. For $\Phi/\Phi_0=0.45$, an antifluxon appears at the central pentagon and four fluxons go through the C60SNW. This is because if the existence of antifluxons were not permitted, all four fluxons should go through the center pentagon because of five-fold symmetry and this fluxon distribution is energetically unstable. Also for $\Phi/\Phi_0=0.20$, total fluxons that go through the C60SNW is $2\Phi_0$ and because of symmetry a $2\Phi_0$ fluxon appears at the central pentagon.

Next, we consider the case where the magnetic field is perpendicular to a hexagon of C60SNW. We show the transition temperature variation with external magnetic field in Fig. 8. The dip and cusp structures appears as in the previous case.

The C60SNW has threefold symmetry around a hexagon. Therefore fluxon distributions of C60SNW, which are shown in Fig. 9, also show this symmetry. For $\Phi/\Phi_0=0.55$, five fluxons go through the C60SNW. Therefore an antifluxon appears at the central hexagon, for the same reasons as in the previous case.

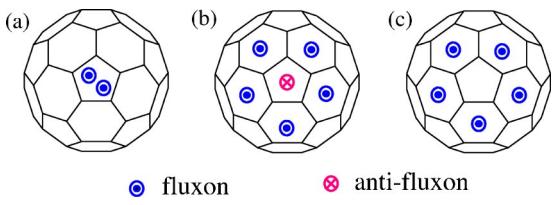

FIG. 7. Top views of the fluxon distribution of C60SNW in the magnetic field perpendicular to a pentagon. Magnitudes of the field corresponds to $\Phi/\Phi_0=0.20$ (a), $\Phi/\Phi_0=0.45$ (b), and $\Phi/\Phi_0=0.60$ (c).

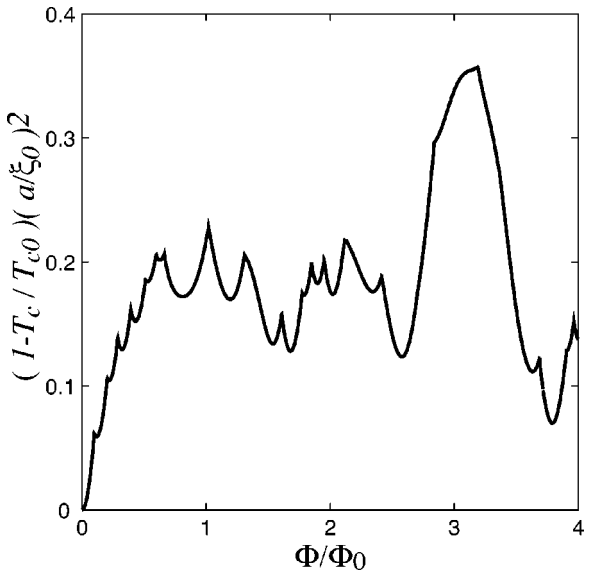

FIG. 8. The magnetic field dependence of the decrease of the transition temperature when the field is perpendicular to a hexagon, where $\Phi = 1.72a^2H$.

This appearance of antifluxons to keep the symmetry of the system is also found in the finite superconducting square lattice networks.[9] An antifluxon also appears in the mesoscopic superconducting plate.[21–23]

In summary, we have studied three-dimensional superconducting networks. In the tetrahedral network, there is rotational symmetry around each of the vertices and superconductivity disappears at the top vertex when the magnetic field is applied along the symmetry axis and $0.25 < \Phi/\Phi_0 < 0.75$. But for C60 networks, there is a rotational symmetry around each of the polygon surfaces and antifluxons appear for keeping the symmetry for the magnetic field parallel to the symmetry axis.

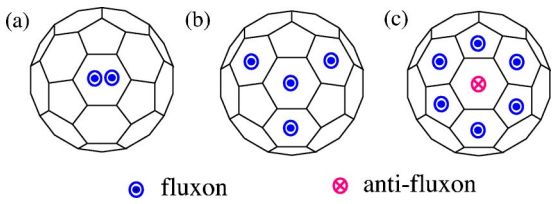

FIG. 9. Top views of the fluxon distribution of C60SNW in the magnetic field perpendicular to a hexagon. Magnitudes of the field correspond to $\Phi/\Phi_0 = 0.25$ (a), $\Phi/\Phi_0 = 0.40$ (b), and $\Phi/\Phi_0 = 0.55$ (c).

These peculiar behaviors show the possibility of application of the three-dimensional superconducting networks as devices controlled by the magnetic field. We hope that progress with the fabrication technique will realize these three-dimensional networks in the near future, especially C60 structures, since this structure is considered to be one of the stable spherical ones.

We thank T. Ishida for fruitful discussions. Also we thank Y. Kayanuma, and other members of quantum physics research group at Osaka Prefecture University.

*Electronic address: gpsato@las.osaka-pct.ac.jp
†Electronic address: kato@ms.osakafu-u.ac.jp

[1] W.A. Little and R.D. Parks, Phys. Rev. Lett. **9**, 9 (1962).
[2] R.D. Parks and W.A. Little, Phys. Rev. **133**, A97 (1964).
[3] P.G. de Gennes, C.R. Seances Acad. Sci., Ser. 2 **292**, 279 (1981).
[4] S. Alexander, Phys. Rev. **27**, 1541 (1983).
[5] J. Simonin, D. Rodrigues, and A. López, Phys. Rev. Lett. **49**, 944 (1982).
[6] H.J. Fink, A. López, and R. Maynard, Phys. Rev. B **26**, 5237 (1982).
[7] R. Rammal, T.C. Lubensky, and G. Toulouse, Phys. Rev. B **27**, 2820 (1983).
[8] *Connectivity and Superconductivity*, edited by J. Berger and J. Rubinstein (Springer, Berlin, 2000).
[9] O. Sato and M. Kato, Phys. Rev. B **68**, 094509 (2003).
[10] J.C.B. Pannetier and R. Rammal, Phys. Rev. Lett. **53**, 1845 (1984).
[11] C.C. Abilio, P. Butaud, T. Fournier, and B. Pannetier, Phys. Rev. Lett. **83**, 5102 (1999).
[12] M.J. Higgins, Y. Xiao, S. Bhattacharya, P.M. Chaikin, S. Sethuraman, R. Bojko, and D. Spencer, Phys. Rev. B **61**, 894(R) (2000).
[13] Y. Xiao, D.A. Huse, P.M. Chaikin, M.J. Higgins, S. Bhattacharya, and D. Spencer, Phys. Rev. B **65**, 214503 (2002).
[14] B. Pannetier, J. Chaussy, and R. Rammal, Jpn. J. Appl. Phys., Suppl. **26**, 1994 (1987).
[15] C. Bonetto, N.E. Israeloff, N. Pokrovskiy, and R. Bojko, Phys. Rev. B **58**, 128 (1998).
[16] T. Puig, E. Rosseel, L.V. Look, M.J.V. Bael, V.V. Moshchalkov, and Y. Bruynseraede, Phys. Rev. B **58**, 5744 (1998).
[17] M. Yoshida, T. Ishida, and K. Okuda, Physica C **357-360**, 608 (2001).
[18] T. Ishida, M. Yoshida, K. Okuda, S.O.M. Sasase, K. Hojou, A. Odawara, A. Nagata, T. Morooka, S. Nakayama, and K. Chinone, Physica C **357-360**, 604 (2001).
[19] M. Yoshida, S. Nakata, and T. Ishida, Supercond. Sci. Technol. **14**, 1166 (2001).
[20] T. Ishida, M. Yoshida, S. Okayasu, and K. Hojou, Supercond. Sci. Technol. **14**, 1128 (2001).
[21] L.F. Chibotaru, A. Ceulemans, V. Bryyndoncx, and V.V. Moshchalkov, Nature (London) **408**, 833 (2000).
[22] V.R. Misko, V.M. Fomin, J. Devreese, and V. Moshchalkov, Phys. Rev. Lett. **90**, 147003 (2003).
[23] L.F. Chibotaru, A. Ceulemans, V. Bruyndoncx, and V. Moshchalkov, Phys. Rev. Lett. **86**, 1323 (2001).